How to cite: *Angew. Chem. Int. Ed.* **2023**, *62*, e202301490
doi.org/10.1002/anie.202301490

Mechanochemistry

The Sonogashira Coupling on Palladium Milling Balls—A new Reaction Pathway in Mechanochemistry

*Wilm Pickhardt, Eleonora Siegfried, Sven Fabig, Marisol Fabienne Rappen, Martin Etter, Maximilian Wohlgemuth, Sven Grätz, and Lars Borchardt**

Abstract: Utilizing direct mechanocatalytical conditions, the Sonogashira coupling was successfully performed on the surface of milling tools by using pure Pd and Pd coated steel balls. The optimization of co-catalyst forming additives led to a protocol, which generates quantitative yields under aerobic conditions for various substrates within as little as 90 minutes. Using state-of-the-art spectroscopic, diffractive, as well as in situ methods lead to the identification of a previously unknown and highly reactive complex of the co-catalyst copper. This new complex differs substantially from the known complexes in liquid phase Sonogashira couplings, proving that reaction pathways in mechanochemistry may differ from those in established synthetic procedures.

Introduction

Mechanochemistry, albeit being in the focus of modern chemists for only a couple of decades, already revolutionized traditional chemistry in numerous aspects.[1] The use of mechanical energy as driving force, inflicted by colliding milling balls, provided greener and faster reactions.[2] Inorganic[3] and organic[4,5] chemistry as well as material science[6] greatly benefited from the use of mechanochemistry. Besides conducting already established reactions in a solvent-free manner, mechanochemistry also offers reaction pathways and mechanisms which sometimes differ from those in liquid phase chemistry, leading to unexpected products.[5,7] Transition metal catalysis is no exception from this as established coupling reactions such as the Heck-, Suzuki-, Negishi- and Sonogashira coupling could be successfully conducted under mechanochemical conditions.[8–10] Typically, the catalyst is used as a salt, and moreover due to the solid-state nature of mechanochemistry frequently without the use of ligands and solvents, already providing an environmental advantage. Yet the catalyst recycling itself is laborious and costly. Particularly in academia, the catalyst is usually discarded after the reaction, limiting the sustainability also of such mechanochemical approaches. Mack et al. provided a great leap towards catalyst recycling as they elaborated a Sonogashira protocol in which the milling tools, i.e., copper ball and vial, functions as co-catalysts.[11] The use of the milling material as active catalysts is referred to as *direct mechanocatalysis*.[12–14] Direct mechanocatalytic reactions offer the advantage that the catalyst can be separated easily from the reaction mixture while offering considerable reaction rate.[12–15] While the work of the Mack group was pioneering this principal, palladium salts were still used as catalyst. Palladium is scarce and laborious to recycle, so we wanted to elaborate on a protocol which utilizes palladium milling balls or even a ball coated with a thin palladium layer as the active catalyst. Developing such an approach and analyzing the impact of the base and co-catalyst forming additives led to a protocol giving high yields with a variety of substrates within 90 minutes (Figure 1). We were able to encounter a previously unknown complex of the copper co-catalyst. The solid-state nature of mechanochemistry allowed for unmatched insights into the co-catalyst formation and composition. The complex differs from the known complexes observed in solution and furthermore, the catalyst proved to be easy to fine-tune so that, in addition to a competitive reaction rate, an insensitivity towards air and moisture could also be achieved.

Results and Discussion

One 10 mm palladium milling ball of approximately 4 g ± 0.3 g was placed into a 19 mL milling vessel manufactured from perfluoroalkoxy alkane (PFA) together with 1 mmol of each starting material and 1 g of potassium carbonate and milled for one hour at 35 Hz in a MM-500.[16] This straightforward approach, using only the starting materials, a base as bulking agent and a Pd milling ball did not lead to the formation of the desired product diphenylacetylene (DA) (cf. Figure 2B, control reaction b1). Estab-

[*] W. Pickhardt, E. Siegfried, Dr. S. Fabig, M. F. Rappen, M. Wohlgemuth, Dr. S. Grätz, Prof. Dr. L. Borchardt
Inorganic Chemistry I,
Ruhr-Universität Bochum
Universitätsstraße 150, 44801 Bochum (Germany)
E-mail: lars.borchardt@rub.de
Dr. M. Etter
Deutsches Elektronen-Synchrotron (DESY)
Notkestraße 85, 22607 Hamburg (Germany)

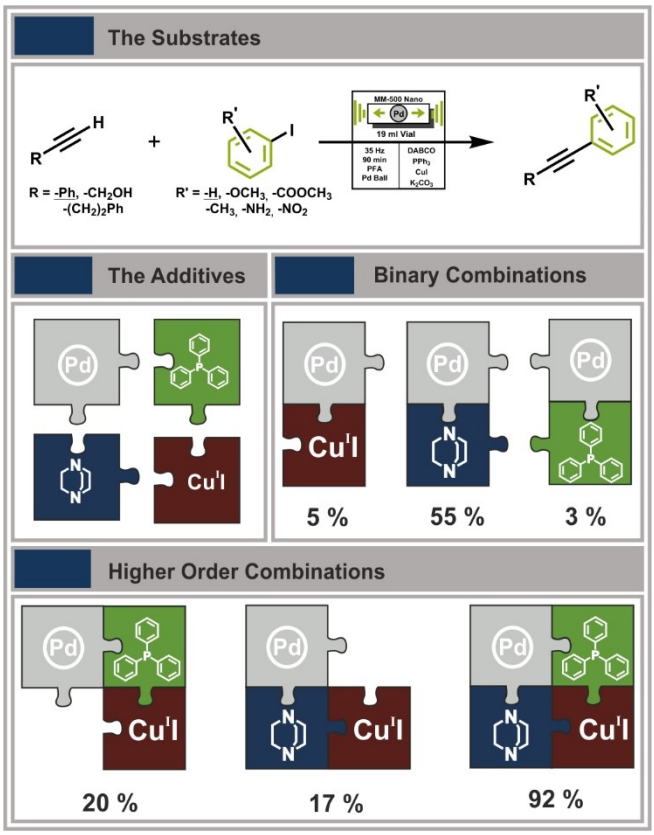

Figure 1. The critical parameters in the direct mechanocatalytic Sonogashira coupling. Standard reaction conditions are highlighted by underlined residues. Although some additives solely lead to successful conversion, only the combination of all three additives and a Pd ball results in an effective coupling.

lished mechanochemical Sonogashira protocols rely on the use of several additives, such as a copper source, amine bases or ligands.[10,17] In the following experiments, we determined the importance of said additives for direct mechanocatalysis by adding them separately to the reaction mixture. In line with the literature, our protocol was first expanded by adding a copper source.[18] After the addition of the co-catalyst, only 5 % of DA could be detected (cf. Figure 2A, Entry 1) as simultaneously the copper-catalyzed competing Glaser reaction took place giving rise to the side product, 1,4-diphenylbutadiyne (DB).[15] Indeed both, other transition metals (cf. Supporting Information, chapter 2.1) and inert atmosphere could suppress this side reaction, but neither led to higher yields even after 12 h milling time.

Glaser side products can entirely be avoided if the Cu co-catalyst is substituted by 1,4-diazabicyclo(2.2.2)octane (DABCO).[9] Using DABCO and a Pd milling ball as the only catalyst lead to yields of 55 % (cf. Figure 2A, Entry 2+3) after one hour and quantitative yields after 4 h (cf. Supporting Information, chapter 2.2.1). To increase the conversion rates further, we began to explore combinations of the additives. CuI and DABCO together, however, performed worse than pure DABCO (cf. Figure 2A, Entry 5), which was surprising as this combination was reported as a catalyst for the conventional solvent-based Sonogashira coupling, already hinting towards the possibility of different reaction pathways under mechanochemical conditions.[19] We further examined the addition of triphenylphosphine (PPh_3), which is a widely applied phosphine ligand in classical liquid phase catalysis and even finds applications as ligand in Cu-catalyzed reactions.[20,21] We could observe trace amounts of DA product formation (cf. Figure 2A, Entry 4). Binary combinations of copper iodide and DABCO or PPh_3 (cf. Figure 2A, Entry 5–8) each led to an insignificant increase in conversion and being worse than the approaches utilizing solely DABCO, but the ternary combination of all additives led to excellent yields of 95 % after 90 minutes of milling (cf. Figure 2A, Entry 8). The protocol using all three additives is also no longer dependent on an inert atmosphere to suppress the Glaser coupling, so further experiments could be performed under air, facilitating sample preparation substantially.

In a next step we aimed to reduce the amount of these additives to a minimum starting from Figure 2A, Entry 8 as benchmark. Our results indicate that DABCO needs to be present in high sub stoichiometric amounts of around 0.3 to 0.6 equiv to achieve high yields (cf. Figure 2C, blue curve). Maintaining these DABCO levels the other additives however can be scaled down to catalytic quantities of 0.5 mol % (cf. Figure 2C, green curve). Substituting DABCO with other amine bases such as triethylamine is feasible (cf. Figure 2B, control reaction b5), but results in slightly lower yields while utilizing more hazardous reagents. Similarly, the CuI can be replaced by CuCl and Cu_2O (cf. Supporting Information, chapter 2.1) which both lead to lower yields.[21,22] Using Cu_2O as a co-catalyst, however, by far outperforms any reported protocols relying on it as a copper source.[21] Nevertheless, CuI was kept as copper source and DABCO as base, as the conversion was the most efficient.

Finally, liquid-assisted grinding (LAG) was tested. Mainly, LAG was intended to counter the problem of the substrates being kneaded into a paste which then sticks to a side of the vial, an effect known as snowballing.[23] This hinders the mass transport during mixing, lowering the yields. In our screening (cf. Supporting Information, chapter 2.3) ethanol, 1,4-cyclooctadiene, 2-butanol and cyclohexane showed an impact on either yield or rheology. We finally settled for the use of cyclohexane in quantities of 0.3 $\mu L\,mg^{-1}$ which resulted in an improved rheology without negatively impacting the yield (cf. Figure 2A, Entry 11).

To rule out rheological influences we continued with the LAG approach and screened substrates of different electronic properties for their efficiency in this coupling. Excellent yields could be generated in as little as 90 minutes with even highly deactivated substrates. Interestingly, polar and aliphatic substrates were proven to react slower in this coupling (cf. Table 1). Even deactivated substrates as well as aniline derivatives show good yields, even though amines are known to bind to copper, which could in theory interfere with the activity of the co-catalyst (cf. Table 1, Entry 5). Under current conditions, brominated or chlorinated substrates, showed no reaction during this screening. In contrast

A Additives Screening

Entry	Additive	Quantity / eq.	Yield
1	CuI	0.8	5 %
2	DABCO	1.2	40 %
3	DABCO	0.6	55 %
4	PPh_3	0.3	3 %
5	DABCO/CuI	0.6/0.8	12 %
6	DABCO/PPh_3	0.6/0.3	27 %
7	CuI/PPh_3	0.8/0.3	20 %
8	CuI/DABCO/PPh_3	0.8/1.2/0.3	95 %
9	CuI/DABCO/PPh_3	0.05/0.6/0.05	94 %
10[a]	CuI/DABCO/PPh_3	0.01/0.6/0.01	83 %
11[b]	CuI/DABCO/PPh_3	0.01/0.6/0.01	84 %
12	CuI/DABCO/PPh_3	0.005/0.6/0.005	67 %

[a] Reaction time was increased to 2 h
[b] Reaction time was increased to 2 h, η 0.3 cyclohexane was added

B Control Reactions

No Additives ***b1*** *- 0 %*	*ZrO_2 Milling Ball* ***b2*** *- 0 %, (0 % DB)*
1.5 eq. KOtBu ***b3*** *- 0%, (22 % DB)*	*$P(tBu)_3 \cdot HBF_4$* ***b4*** *- 78 %*
0.6 eq. Triethylamine ***b5*** *- 78 %*	

C Additives Permutation

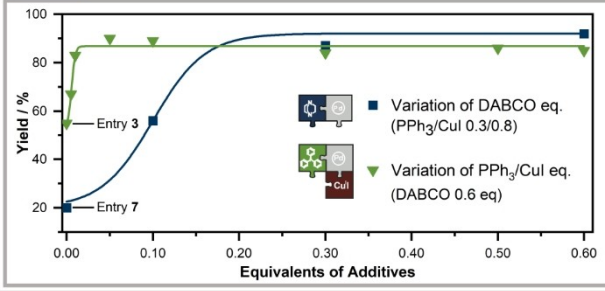

Figure 2. A) Summary of the performed additives testing and control experiments (B). All reactions were performed using 112 µL iodobenzene (1 mmol, 204 mg), 132 µL phenylacetylene (1.2 mmol, 123 mg) and 1.0 g potassium carbonate (K_2CO_3, 7.24 mmol) under inert atmosphere in a 19 mL PFA vessel with one Pd ball and milling for 60 min at 35 Hz in a MM500. Yield determined by HPLC. C) Variation of dabco at constant amounts of PPh_3/CuI (blue squares) and variation of PPh_3/CuI at constant amounts of dabco (green triangle). The complex-forming additives can be scaled down to as little as 5 or even 0.5 mol% to reach 90% or 67% conversion, respectively. Detailed informations are to be found in Supporting Information, chapter 2.2.2.

Table 1: Summary of the performed substrate screening. All reactions were performed according to Figure 2 Entry 9 in 19 mL PFA vessels at 35 Hz for 90 min with 1 mmol of each starting material and 1 g potassium carbonate.

A Substrate Screening

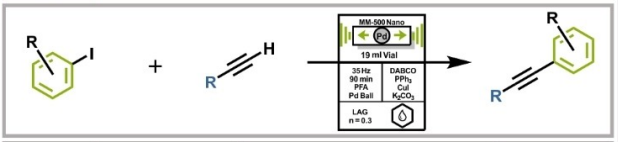

Entry	R	R-Alkyne	Yield
1	-H		94 %[a]
2	4-OMe		98 %[b]
3	4-COOMe		>99 %[b]
4	4-NO_2		>99 %[b]
5	4-NH_2		85 %[b]
6	4-Me		>99% %[b]
7	-H	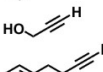	68 %[b]
8	-H	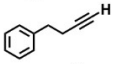	99 %[b]
9			20 %[b]

[a] Isolated yields are reported
[b] Yield determined by ^1H NMR using dibromomethane as internal standard.

to previous studies[16] the use of potassium iodide, intended to carry out a trans halogenation, did not lead to a successful coupling of brominated substrates.

Being aware that utilizing pure Pd balls as catalysts is costly, we applied a direct mechanocatalytic protocol elaborated in our group to this coupling which utilizes electroplated steel balls, lowering the catalyst ball costs significantly.[24] The experiments were carried out according to Figure 2A, Entry 10. After 5 cycles the reactivity remained unchanged, which highlights the capability of the electroplated balls, even though the electroplated milling balls showed consistently slightly lower yields than pure Pd balls (cf. Supporting Information, chapter 5).

After the additives and their role in this reaction were identified and the method was tested for its versatility, we wanted to investigate how these additives interact and lead to this astonishing reaction rates once combined in the right stoichiometry. First, we directed our attention to the PPh_3 and investigated its role with several spectroscopic methods, utilizing the refined reaction conditions (cf. Figure 2A, Entry 9). We can show by X-ray photoelectron spectroscopy (XPS) that Pd in its form of a milling ball is not able to form a molecular $Pd(PPh_3)_4$ complex (cf. Supporting Information, chapter 4.5).[16] Next, nuclear magnetic resonance spectra (NMR) of the phosphorus were recorded. ^{31}P NMR spectra were recorded from the milled mixture washed with $CDCl_3$ directly after milling. The absence of any phosphorus signals indicates that the phosphine must be bound in an insoluble compound, and not in a typical homogeneous Pd complex (cf. Supporting Information, chapter 4.4). This is further reinforced by the low amount of Pd abrasion of less than 1 µg within one hour (cf. Supporting Information, chap-

ter 4.4.1) and the low activity of the protocol with only PPh_3 as additive (cf. Figure 2A, Entry 4). To further exclude the possibility of PPh_3 acting as surface-bound ligand, cyclisation experiments were done which ultimately showed that the ligand does not bind to the Pd ball (cf. Supporting Information, chapter 2.4). The XPS investigations of the milled mixture showed that the PPh_3 signals shift in the procedure (cf. Supporting Information, chapter 4.5).

This is further corroborated by powder X-ray diffraction (PXRD), where during milling, new reflexes appear which are neither present in the starting materials nor possible products of this reaction (cf. Supporting Information, chapter 4.3). Together, these investigations pointed towards a crystalline Pd-free complex of the co-catalyst which is formed during milling. Attempts were made to obtain crystal structure data of the formed copper complex, but were not successful (cf. Supporting Information, chapter 4.3.1).

Therefore, Raman spectroscopy investigations targeting the stoichiometry of the milled mixture were performed to get a deeper insight into the complex stoichiometry and structure. Here, a shift of the C–C triple bond from 2125 cm^{-1} in pure phenylacetylene to 2035 cm^{-1} in the milled mixture was observed, proving that the phenylacetylene is part of the formed co-catalyst complex (cf. Supporting Information, chapter 4.1, Figure 3A + B, Complex **I**). Reference experiments utilizing a strong base, potassium tert-butoxide (KO*t*Bu) showed that this shift is not due to an end-on copper complex, but rather a side-on coordination (cf. Figure 2B, control experiment b3, Figure 3A, Supporting Information, chapter 4.1.2 + 4.1.3).

After isolating the participating components, we synthesized the complex in absence of the aryl iodine and potassium carbonate by milling everything together stoichiometrically for 30 min at 35 Hz. This resulted in a light-yellow powder, which exclusively show the previously discovered Raman shift, indicating a quantitative complex formation. Further investigations showed that the additives can be added to the phenylacetylene regardless of order and will always result in complex **I** to be formed (cf. Figure 3A + B, Supporting Information, chapter 4.1.2 + 4.1.3). During these investigations we could even identify a second copper complex with a characteristic C–C triple bond signal at 1940 cm^{-1} when only CuI, phenylacetylene and DABCO are milled together (cf. Figure 3C, Complex **II**). However, this complex shows a low reactivity (cf. Figure 2A, Entry 5). Adding PPh_3 to this complex leads to a complete conversion to complex **I** (cf. Figure 3C, Supporting Information, chapter 4.1.3).

To investigate the previously observed Raman shift, density-functional theory (DFT) calculations with regards to the used additives and their stoichiometry were used to simulate a Raman spectrum of a possible complex formed from CuI, DABCO phenylacetylene and PPh_3 (cf. Supporting Information, chapter 4.1.2). The calculated relative Raman shift position observed for phenylacetylene and the shifts of the triple bond with varying additives match the obtained spectroscopic data. Common complexes observed in the Sonogashira coupling or an end-on coordinated,

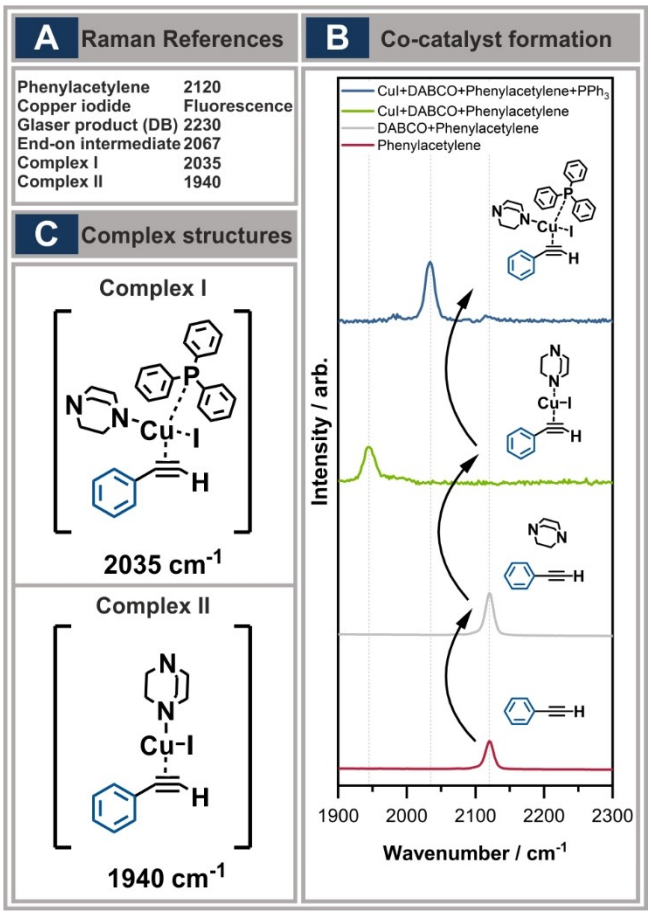

Figure 3. A) Raman shift reference values of different alkyne compounds and complex components discussed during this investigation. B) Sequential addition of co-catalyst forming additives, starting from phenylacetylene and DABCO in the first step. No alternation of the triple bond signal was observed. After addition of CuI the signal of the triple bond shifted towards 1940 cm^{-1}, indicating that a phenylacetylene incorporating complex II was formed. After the addition of PPh_3, the triple bond signal shifts to 2035 cm^{-1} forming complex. Detailed discussions of further sequences are to be found in Supporting Information, chapter 4.1.3. C) Co-catalyst structures obtained by DFT calculations.

deprotonated species would not show any shift (cf. Supporting Information, chapter 4.1.1–4.1.3).

To shed light onto the time-related procedure of the catalysis, two powerful in situ techniques were utilized. First, in situ Raman spectroscopy was done which confirmed our assumption of a co-catalyst complex to be formed from phenylacetylene and the additives. This complex in turn is converted into the Sonogashira coupling product, which can be seen on the shift of the C–C triple bond during the reaction (cf. Supporting Information, chapter 4.1.4). Advancing even further and exploiting the crystalline nature of the suspected co-catalyst species, in situ XRD experiments were carried out (Figure 4). The analysis revealed the reflection associated with the co-catalyst complex **I** are formed in the first minutes of the reaction and coincide with the fast consumption of CuI, which is finished after only 10 minutes. Over time, these reflections start to vanish with

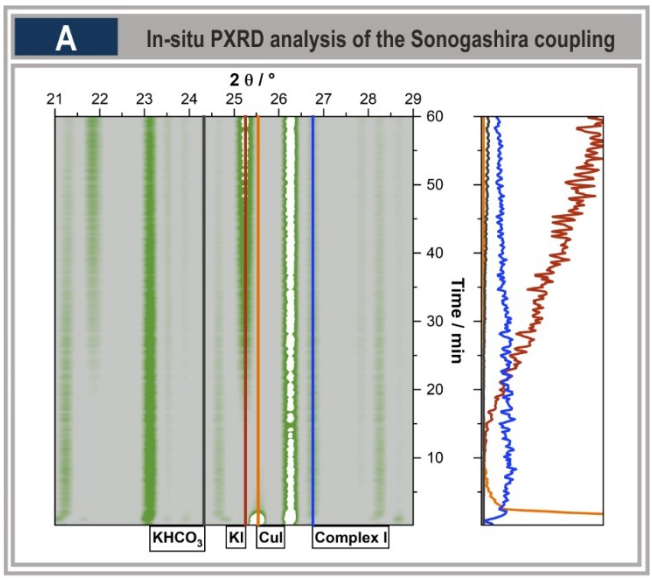

Figure 4. In situ PXRD diffractogram. At first, the CuI reflection (orange) shows high intensity which vanishes completely during proceeding of the reaction. At the same time, the reflection of the co-catalyst (blue), which is not present from the beginning, rises sharply and decrease due to its consumption in the reaction. KI (red), which is the necessary by-product of a succesful reaction arises after 10 minutes. Likewise, reflection of the protonated base ($KHCO_3$, dark grey line) becomes observable proving the succesful reaction. A wavelength of 0.20731 nm was utilized to obtain the diffractograms. For better comparability, the reflections were recalculated to the wavelength of Cu Kα1 radiation ($\lambda = 1.5406$ Å). Detailed diffractograms and discussion of the procedure are given in Supporting Information, chapter 4.3.2.

simultaneous occurrence of the product reflections. Both previously elaborated structures (cf. Figure 3C) were shown to be formed by this principle and generate the product, with complex **I**, featuring PPh_3, outperforming complex **II** significantly (cf Figure 4, Supporting Information, chapter 4.3.2). It became apparent that DABCO indeed is part of the formed complex and does not deprotonate the acetylene, which can be seen on the formed KI reflection as well as on the slowly emerging $KHCO_3$ reflection. These experiments confirm our previous results and prove not only the course of the reaction and highlight the importance of PPh_3, but also show which component is the active base, being K_2CO_3. In typical liquid-phase Sonogashira coupling, the copper first binds side-on to the phenylacetylene which is subsequently deprotonated by an amine base, leading to an end-on complex which then undergoes the transmetalation. In this mechanocatalytic protocol, however, this is not the case. The amine base DABCO does not deprotonate the acetylene, as this would lead to an immediate formation of DB, which is not observed when DABCO, CuI and phenylacetylene are milled together (cf. Figure 2B, reference experiment b3, Figure 3B).

Ultimately, the combination of these powerful spectroscopic tools provided the following information:

1) Copper, DABCO and PPh_3 are part of the complex of the co-catalyst.
2) Copper, DABCO as well as the phosphine undergo an electronic change.
3) The acetylene moiety remains protonated and is part of a complex, formed from one equivalent DABCO, PPh_3 and a copper atom which is bound side-on to the acetylene.

Conclusion

Regarding the goal of performing a Sonogashira coupling under direct mechanocatalytic conditions, a facile, sustainable, and fast protocol for the Sonogashira was developed. This can be performed with Pd balls as well as with coated steel balls. Furthermore, and less included in the initial objective of our work, we found that under mechanochemical conditions, intermediates and reaction pathways can occur that are substantially different from those in established chemistry. This study highlights how mechanochemistry can provide insights into reaction mechanisms and intermediates directly from the reaction mixture. The complex of the co-catalyst, which enables this fast coupling was investigated. Even though single-crystal data could not be obtained, the complex structure was elucidated by experiments proving the molecular composition with subsequent analysis of the complex. The data was compared to spectra obtained from DFT calculations, proving the structures. The complex found during this work differs from the typical copper complex found in the Sonogashira coupling (cf. Figure 3C, Supporting Information, chapter 4.1.2–4.1.3). Furthermore, we tested the capability of our system on various substrates with different electronic properties (cf. Table 1). Our results show the versatility of the approach which can generate excellent yields with various starting material combinations. A general trend is seen that more polar and aliphatic starting materials react slower in this coupling and even typical catalyst poisoning substrates such as primary amines can be coupled. Brominated and chlorinated substrates, however, do not show any conversion in the direct mechanocatalytic Sonogashira coupling under the given conditions.

Acknowledgements

Special thanks go to Miriam Sander for the obtained X-ray diffractograms and patience regarding numerous demanded XRD measurements during these investigations. Furthermore, we want to thank the team of SolidChem GmbH, Bochum, Germany, especially Dominique Gopalakrishnan, for measuring the needed high-resolution XRD diffractograms. We further gratefully acknowledge Prof. Dr. Uwe Ruschewitz for structure elucidation via powder Xray diffraction. We acknowledge DESY (Hamburg, Germany), a member of the Helmholtz Association HGF, for the provision of experimental facilities. Parts of this research were carried out at PETRA III beamline P02.1. Beamtime was allocated by an in-house contingent. We gratefully acknowledge the funding from the European Research

Council (ERC) under the European Union's Horizon 2020 research and innovation programme ("Mechanocat", grant agreement No 948521). Open Access funding enabled and organized by Projekt DEAL.

Conflict of Interest

The authors declare no conflict of interest.

Data Availability Statement

The data that support the findings of this study are available from the corresponding author upon reasonable request.

Keywords: Ball Milling · Cross-Coupling · Mechanocatalysis · Transition Metal Catalysis · in Situ Characterization

[1] a) S. L. James, T. Friščić, *Chem. Soc. Rev.* **2013**, *42*, 7494; b) G.-W. Wang, *Chem. Soc. Rev.* **2013**, *42*, 7668; c) L. Takacs, *Chem. Soc. Rev.* **2013**, *42*, 7649.
[2] K. J. Ardila-Fierro, J. G. Hernández, *ChemSusChem* **2021**, *14*, 2145.
[3] D. Tetzlaff, K. Pellumbi, D. M. Baier, L. Hoof, H. Shastry Barkur, M. Smialkowski, H. M. A. Amin, S. Grätz, D. Siegmund, L. Borchardt, *Chem. Sci.* **2020**, *11*, 12835.
[4] D. M. Baier, S. Grätz, B. F. Jahromi, S. Hellmann, K. Bergheim, W. Pickhardt, R. Schmid, L. Borchardt, *RSC Adv.* **2021**, *11*, 38026.
[5] W. Pickhardt, M. Wohlgemuth, S. Grätz, L. Borchardt, *J. Org. Chem.* **2021**, *86*, 14011.
[6] a) A. Krusenbaum, J. Geisler, F. J. L. Kraus, S. Grätz, M. V. Höfler, T. Gutmann, L. Borchardt, *J. Polym. Sci.* **2022**, *60*, 62; b) T. Rensch, V. Chantrain, M. Sander, S. Grätz, L. Borchardt, *ChemSusChem* **2022**, *15*, e202200651.
[7] J. G. Hernández, C. Bolm, *J. Org. Chem.* **2017**, *82*, 4007.
[8] a) J. Yu, H. Shou, W. Yu, H. Chen, W. Su, *Adv. Synth. Catal.* **2019**, *361*, 5133; b) S. Grätz, B. Wolfrum, L. Borchardt, *Green Chem.* **2017**, *19*, 2973; c) F. Schneider, A. Stolle, B. Ondruschka, H. Hopf, *Org. Process Res. Dev.* **2009**, *13*, 44; d) Q. Cao, J. L. Howard, E. Wheatley, D. L. Browne, *Angew. Chem. Int. Ed.* **2018**, *57*, 11339.
[9] R. Thorwirth, A. Stolle, B. Ondruschka, *Green Chem.* **2010**, *12*, 985.
[10] D. A. Fulmer, W. C. Shearouse, S. T. Medonza, J. Mack, *Green Chem.* **2009**, *11*, 1821.
[11] R. A. Haley, J. Mack, H. Guan, *Inorg. Chem. Front.* **2017**, *4*, 52.
[12] S. Hwang, S. Grätz, L. Borchardt, *Chem. Commun.* **2022**, *58*, 1661.
[13] W. Pickhardt, S. Grätz, L. Borchardt, *Chem. Eur. J.* **2020**, *26*, 12903.
[14] C. G. Vogt, S. Grätz, S. Lukin, I. Halasz, M. Etter, J. D. Evans, L. Borchardt, *Angew. Chem. Int. Ed.* **2019**, *58*, 18942.
[15] C. G. Vogt, M. Oltermann, W. Pickhardt, S. Grätz, L. Borchardt, *Adv. Energy Sustainability Res.* **2021**, *2*, 2100011.
[16] W. Pickhardt, C. Beaković, M. Mayer, M. Wohlgemuth, F. J. Leon Kraus, M. Etter, S. Grätz, L. Borchardt, F. J. L. Kraus, *Angew. Chem. Int. Ed.* **2022**, *61*, e202205003.
[17] Y. Liang, Y.-X. Xie, J.-H. Li, *J. Org. Chem.* **2006**, *71*, 379.
[18] M. Schilz, H. Plenio, *J. Org. Chem.* **2012**, *77*, 2798.
[19] J.-H. Li, J.-L. Li, D.-P. Wang, S.-F. Pi, Y.-X. Xie, M.-B. Zhang, X.-C. Hu, *J. Org. Chem.* **2007**, *72*, 2053.
[20] a) B. Soberats, L. Martínez, M. Vega, C. Rotger, A. Costa, *Adv. Synth. Catal.* **2009**, *351*, 1727; b) J. T. Guan, G.-A. Yu, L. Chen, T. Qing Weng, J. J. Yuan, S. H. Liu, *Appl. Organomet. Chem.* **2009**, *23*, 75.
[21] Y. Nishihara, S. Noyori, T. Okamoto, M. Suetsugu, M. Iwasaki, *Chem. Lett.* **2011**, *40*, 972.
[22] F. Monnier, F. Turtaut, L. Duroure, M. Taillefer, *Org. Lett.* **2008**, *10*, 3203.
[23] M. Carta, S. L. James, F. Delogu, *Molecules* **2019**, *24*, 3600.
[24] M. Wohlgemuth, M. Mayer, M. Rappen, F. Schmidt, R. Saure, S. Grätz, L. Borchardt, *Angew. Chem. Int. Ed.* **2022**, *61*, e202212694.

Manuscript received: January 30, 2023
Accepted manuscript online: April 5, 2023
Version of record online: May 25, 2023